scientific reports

Check for updates

OPEN

Comparison of crosslinked and non-crosslinked collagenated xenografts for vertical bone augmentation in rabbit calvaria

Hee-seung Han[1,5], Hyunkyung Kim[2,5], Narasaem Lee[3], Semin Kim[4], Sungtae Kim[2] & Young-Dan Cho[2]✉

Bovine or porcine xenografts, which are readily available and possess osteoconductivity, are widely used for bone augmentation in clinical practice. The addition of collagen to particulated bone graft material improves handling characteristics and helps maintain graft integrity. These collagenated bone, when collagen is appropriately cross-linked, provide enhanced osteogenic potential and structural stability. However, studies on the histological changes due to the use of collagenated bovine bone for vertical bone augmentation are lacking. Therefore, this study aimed to compare the osteoconductivity and volume stability of two collagenated xenografts—deproteinized bovine bone mineral (DBBM) with crosslinked bovine collagen (DBBM-Cb; A-Oss Collagen) and non-crosslinked porcine collagen (DBBM-NCp; Bio-Oss Collagen)—using rabbit calvarial models of vertical augmentation and critical-sized defects. Surface morphology of the grafts was analyzed using field emission scanning electron microscopy. In vivo bone regeneration was assessed using micro-computed tomography and histological analyses at 3, 5, 6, and 12 weeks following bone grafting in calvarial vertical-augmentation and defect models. Both grafts showed porous and interconnected microarchitecture favorable for osteoconduction. In the augmentation model, DBBM-Cb demonstrated significantly higher bone volume fraction (bone volume/total volume of bone tissue) at 3 weeks and vertical height retention at both 3 and 5 weeks ($P < 0.05$). In the defect model, DBBM-Cb led to significantly greater defect closure at 12 weeks ($P < 0.05$). Histological analyses confirmed improved graft integration and bone maturation with DBBM-Cb. DBBM-Cb exhibited superior osteoconductivity, structural stability, and graft volume maintenance compared to DBBM-NCp. These properties support its potential as a more effective biomaterial for vertical bone augmentation.

Keywords Animal model, Bone substitutes, Collagen, Histology, Rabbit, Xenograft

Extensive bone augmentation is required when the vertical bone height is insufficient for implant placement. Although autogenous bone graft is recommended because of its high osteoinductive capacity, its clinical application is often limited by donor site morbidity, restricted availability, and significant graft resorption[1,2]. Therefore, bovine or porcine xenografts, which are readily available and possess osteoconductivity, are widely used in clinical practice[3–5]. However, to achieve successful vertical bone augmentation, stabilization devices, such as titanium meshes, membranes, and tacks, are required to maintain the integrity of these particulate bone-graft materials[6–8].

To enhance the stability of the graft after bone augmentation, collagen can be incorporated into the particulated bone graft material, which facilitates easier handling during surgery while preserving structural integrity[9]. These collagenated bone grafts contain type I collagen, the main extracellular matrix component in bone, which serves as a scaffold to promote osteoblast migration, angiogenesis, and new bone formation[10]. Owing to its fibrillar structure, collagen incorporated into bovine or porcine bone-graft materials enhances clot

[1]Department of Periodontology, Korea University Anam Hospital, Seoul, Republic of Korea. [2]Department of Periodontology, School of Dentistry and Dental Research Institute, Seoul National University and Seoul National University Dental Hospital, 101 Daehak-no, Jongno-gu, Seoul 03080, Republic of Korea. [3]Bone Science Evaluation Team, Tissue Regeneration Institute, Osstem Implant Co. Ltd., Seoul, Republic of Korea. [4]Xenograft Development Team, Tissue Regeneration Institute, Osstem Implant Co. Ltd., Seoul, Republic of Korea. [5]Hee-seung Han and Hyunkyung Kim contributed equally as first authors. ✉email: cacodm1@snu.ac.kr

preservation, provides a scaffold for cellular infiltration, and improves the adaptability of the graft to the defect site, thereby optimizing bone-regeneration outcomes[11].

However, collagenase rapidly degrades the organic component of collagenated bone applied in vivo. For optimal bone regeneration, maintaining the collagen-matrix volume for a sufficient duration is imperative to support the adhesion and formation of new bone on the graft material[12], and chemical crosslinking techniques are frequently used to control the degradation rate[13]. Appropriately crosslinked collagen scaffolds can achieve high osteogenic potential and structural stability[14], as the crosslinked matrix resists degradation by collagenase and prevents fibroblast infiltration through the structure[15,16]. However, the degree of endogenous crosslinking in collagen varies according to the source animal, and concealed collagenase cleavage sites potentially affect the degradation rate[17].

However, studies on the histological changes due to the use of collagenated bovine bone for vertical bone augmentation, particularly when the origin and properties of collagen are altered, are lacking. Therefore, this in vivo study aimed to compare the new bone regeneration rate of xenografts with crosslinked and non-crosslinked collagen matrices. Two commercially available xenogeneic bone graft materials were evaluated: (1) deproteinized bovine bone mineral with 10% crosslinked bovine collagen (DBBM-Cb; A-Oss Collagen, Osstem, Seoul, Republic of Korea) and (2) deproteinized bovine bone mineral with 10% non-crosslinked porcine collagen (DBBM-NCp; Bio-Oss Collagen, Geistlich Pharma, Wolhusen, Switzerland). These materials were selected because both are widely used in clinical practice, yet their collagen components differ in crosslinking and origin, which may influence graft stability and biological performance. To compare their osteoconductive potential, two distinct rabbit calvarial models were employed: vertical bone augmentation and defect model, followed by micro-CT and histological evaluation at multiple time points. The null hypothesis was that there would be no significant difference in volume stability or new bone formation between DBBM-Cb and DBBM-NCp. Rejection of null hypothesis would indicate that there was a significant difference in volume stability or new bone formation between DBBM-Cb and DBBM-NCp.

Results

Twenty-four male New Zealand White rabbits were used in this study and all survived to the designated endpoints with no surgical complications. Animals typically recovered from anesthesia within ~1 h, and all wounds healed uneventfully. All 24 animals were included in the analysis, yielding n = 6 per group/time point (defect model: 6 and 12 weeks; augmentation model: 3 and 5 weeks). No animals were excluded due to outlier observations, complications, or premature death.

Characteristics of collagenated bone graft materials

Figure 1 presents the FE-SEM images of DBBM-Cb and DBBM-NCp at different magnifications, highlighting their surface morphology and microstructural characteristics. Both DBBM-Cb and DBBM-NCp exhibited a highly porous structure, which is essential for cell infiltration and osteoconduction. DBBM-Cb had a defined and interconnected porous network, suggesting enhanced permeability for biological fluids and cellular migration. Both materials exhibited a well-organized collagen-fiber structure with distinctive alignments, potentially contributing to better mechanical stability and cell attachment.

Bone formation and residual graft maintenance in the calvarial augmentation model

Figure 2A shows the areas grafted with DBBM-Cb and DBBM-NCp at postoperative 3 and 5 weeks (Supplementary Videos S1–S4). Compared to DBBM-NCp, DBBM-Cb demonstrated a more stable and structured augmentation over time, with lesser volume reduction. The bone volume fraction (bone volume [BV]/total volume of bone tissue [TV]) at 3 weeks was significantly higher in the DBBM-Cb group than in the DBBM-NCp group ($P < 0.05$; Fig. 2B), indicating substantially greater early bone formation. At 5 weeks, BV/TV remained higher in the DBBM-Cb group; however, the difference was less pronounced. At both 3 and 5 weeks, the reduction in vertical graft height in the 3 M DBBM-NCp group was significantly greater than that in the DBBM-Cb group ($P < 0.05$; Fig. 2C). This suggests that DBBM-Cb maintains its structure more effectively over time.

Bone formation in the calvarial defect model

Figure 3A presents representative micro-CT images of bone defects treated with DBBM-Cb and DBBM-NCp at 6 and 12 weeks post-surgery (Supplementary Videos S5–S8). Over time, both materials induced progressive defect closure. Figure 3B presents the percentage of defect closure at postoperative 6 and 12 weeks. At 6 weeks, the mean defect closure percentage was higher in the DBBM-Cb group than in the DBBM-NCp group; however, the difference was not statistically significant. By 12 weeks, the DBBM-Cb group exhibited significantly greater defect closure compared to the DBBM-NCp group ($P < 0.05$), indicating enhanced bone regeneration and healing over time.

Histological analysis of augmented bone tissues

Figure 4 presents histological sections of vertically augmented bone tissues at 3 and 5 weeks post-surgery. At 3 weeks, distinct differences were observed between the DBBM-Cb and DBBM-NCp groups in terms of collagen scaffold persistence and new bone formation. In the DBBM-Cb group, substantial amounts of residual collagen (Fig. 4, asterisks) were consistently noted across all regions.

In the DBBM-Cb group, the upper regions demonstrated a more consolidated bone matrix with maintained DBBM at 5 weeks. In the lower regions, both groups exhibited greater osteoid deposition and connectivity between new and host bone.

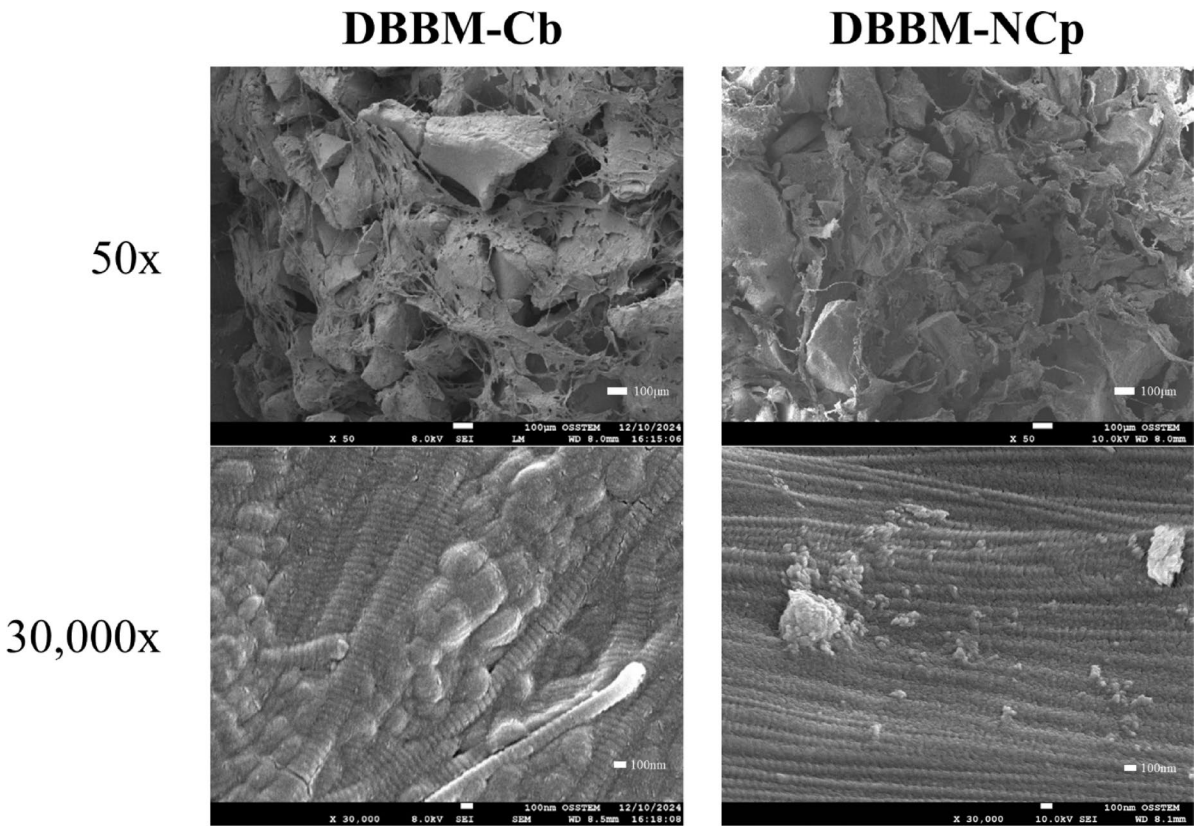

Fig. 1. Comparison of characteristics of two collagenated bone grafts. Representative field emission scanning electron microscopy images at magnifications of 50×, and 30,000× showing the microstructural characteristics of the two materials. *DBBM-NCp* deproteinized bovine bone mineral with non-crosslinked porcine collagen (Bio-Oss Collagen, Geistlich Pharma, Switzerland), *DBBM-Cb* deproteinized bovine bone mineral with crosslinked bovine collagen (A-Oss Collagen, Osstem, Republic of Korea).

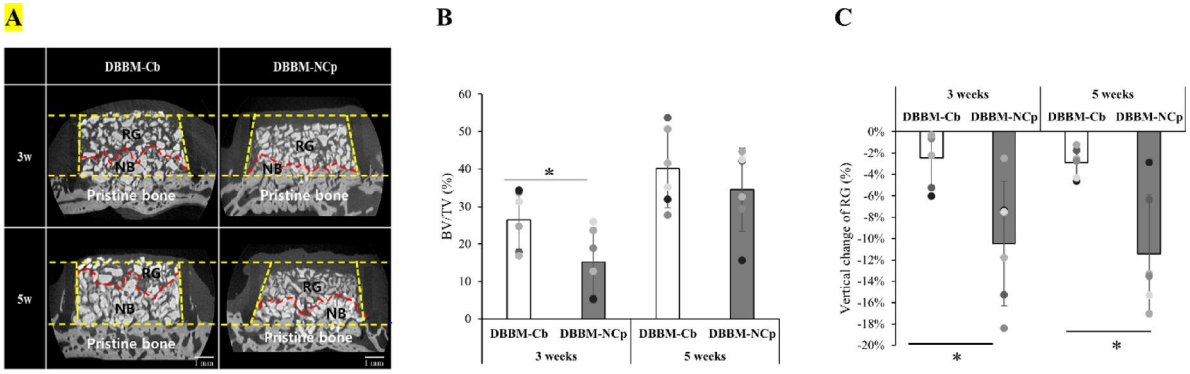

Fig. 2. Evaluation of bone formation and residual graft maintenance in calvarial augmentation model. (**A**) Representative microcomputed tomography images of calvarial bone-graft sites at 3 and 5 weeks after surgery in the DBBM-Cb and DBBM-NCp groups. Yellow dotted lines indicate the boundaries of the guide tube, and red dotted lines represent the boundary between newly formed bone and residual graft material. (**B**) Bone volume fraction (BV/TV, %) of the augmented regions at 3 and 5 weeks. The DBBM-Cb group demonstrates significantly higher BV/TV than DBBM-NCp at 3 weeks ($P < 0.05$). (**C**) Vertical change in residual graft (RG) height (%) at 3 and 5 weeks. The DBBM-Cb group shows significantly less vertical reduction compared to DBBM-NCp at both time points ($P < 0.05$). *BV* bone volume, *TV* total volume of bone tissue, *DBBM-NCp* deproteinized bovine bone mineral with non-crosslinked porcine collagen (Bio-Oss Collagen, Geistlich Pharma, Switzerland), *DBBM-Cb* deproteinized bovine bone mineral with crosslinked bovine collagen (A-Oss Collagen, Osstem, Republic of Korea).

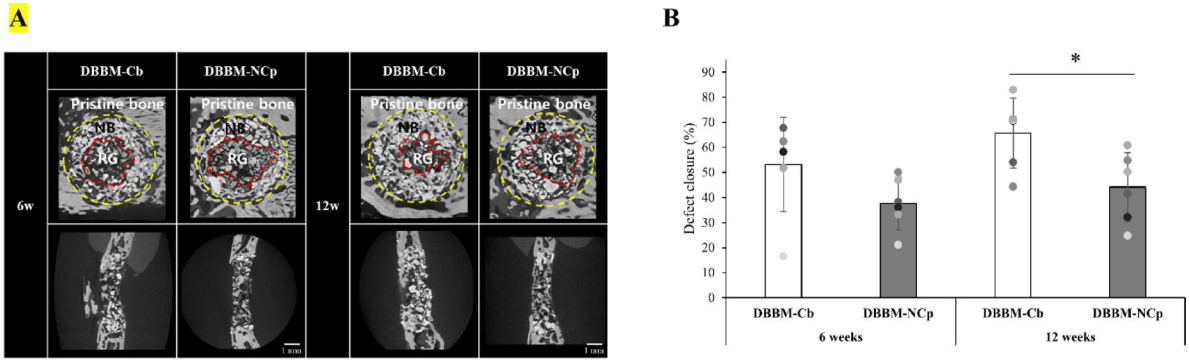

Fig. 3. Evaluation of bone formation in calvarial defect model. (**A**) Representative microcomputed tomography images of calvarial critical-sized defects treated with DBBM-Cb and DBBM-NCp at 6 and 12 weeks after surgery. The region of interest (yellow dotted lines) was defined as the area surrounding the guide tube in the defect area in the calvarial defect model. Red dotted lines represent the boundary between newly formed bone and residual graft material. (**B**) Quantitative analysis of defect closure (%) at 6 and 12 weeks. DBBM-Cb demonstrates significantly greater defect closure than DBBM-NCp at 12 weeks ($P < 0.05$). *DBBM-NCp* deproteinized bovine bone mineral with non-crosslinked porcine collagen (Bio-Oss Collagen, Geistlich Pharma, Switzerland); DBBM-Cb, deproteinized bovine bone mineral with crosslinked bovine collagen (A-Oss Collagen, Osstem, Republic of Korea).

Histological analysis of the defect site

At 6 weeks, both DBBM-Cb and DBBM-NCp groups demonstrated bone regeneration along the periphery of the grafted region. In the DBBM-Cb group, newly formed bone tissue was observed interspersed between the graft particles, with evidence of vascular infiltration and residual collagen (Fig. 5A).

At 12 weeks, the DBBM-Cb group exhibited more advanced bone maturation with trabecular bone structures evident throughout the grafted region. New bone was in close contact with the residual graft particles, indicating active bone remodeling (Fig. 5B).

Discussion

This study provides compelling evidence that compared with DBBM-NCp, DBBM-Cb provides better outcomes regarding several key aspects of bone regeneration. A comprehensive analysis of the physicochemical properties and in vivo performance revealed that DBBM-Cb combines favorable structural, mechanical, and biological characteristics that contribute to enhanced osteoconduction and long-term graft stability.

Vertical ridge augmentation is often limited by the lack of surrounding bone walls, and the graft is prone to resorption. Conventional guided bone regeneration techniques using titanium meshes or block autografts can address this but are associated with increased surgical complexity and risks[18,19]. As an alternative, collagen-xenograft composites, such as DBBM-Cb, help maintain structural integrity while promoting angiogenesis and cell migration and minimizing the need for additional grafting[12].

These findings align with previous reports suggesting that improved graft integration and remodeling are critical for successful bone regeneration and long-term clinical success[20,21]. Collagenated xenogeneic bone grafts enhance new bone formation, enhance integration between graft particles, and achieve successful implant stability[22,23]. Additionally, compared to particulate bone grafts, the maximum resorption measures for collagenated xenografts are lower by > 50% than those for particulate bone grafts, indicating considerably better vertical ridge preservation[24].

DBBM-NCp, widely used in clinical practice for its biocompatibility and angiogenic potential, has shown reliable outcomes in augmentation procedures[25,26]. However, its degradation characteristics raises concerns about long-term volume stability, and evidence on volumetric persistence remains limited. Collagenation improves handling, hemostasis[27], and space maintenance[28] but may add cost and introduce collagen-dependent resorption kinetics[29]. In the present study, the superior bone regeneration observed in the DBBM-Cb group may be attributed to prolonged collagen stability (Figs. 4 and 5). Enzymatic degradation assays showed that DBBM-Cb retained 42% of its collagen after 72 h, whereas DBBM-NCp underwent complete degradation within 24 h[30]. The prolonged presence of residual collagen may help preserve the structural integrity of the defect site and provide a long-lasting osteoconductive scaffold. Although the degree of bone maturation observed at the early stage was relatively low, the persistent matrix could facilitate sustained bone regeneration over time by providing a stable environment conducive to cellular infiltration and extracellular matrix deposition. Moreover, the slow degradation rate helps preserve graft volume and provides mechanical stability during critical phases of bone healing. Such structural persistence is particularly advantageous in clinical contexts where long-term space maintenance is essential, such as vertical or large-volume bone augmentation procedures.

The enhanced performance of DBBM-Cb may be related to its material origin[14] and degree of collagen crosslinking. Although porcine collagen typically degrades faster than bovine collagen[31,32], crosslinking—either natural or chemically induced—can extend scaffold longevity[33,34], aiding bone regeneration. Considering the prolonged stability and resistance to enzymatic degradation observed in DBBM-Cb, its potential as a scaffold for

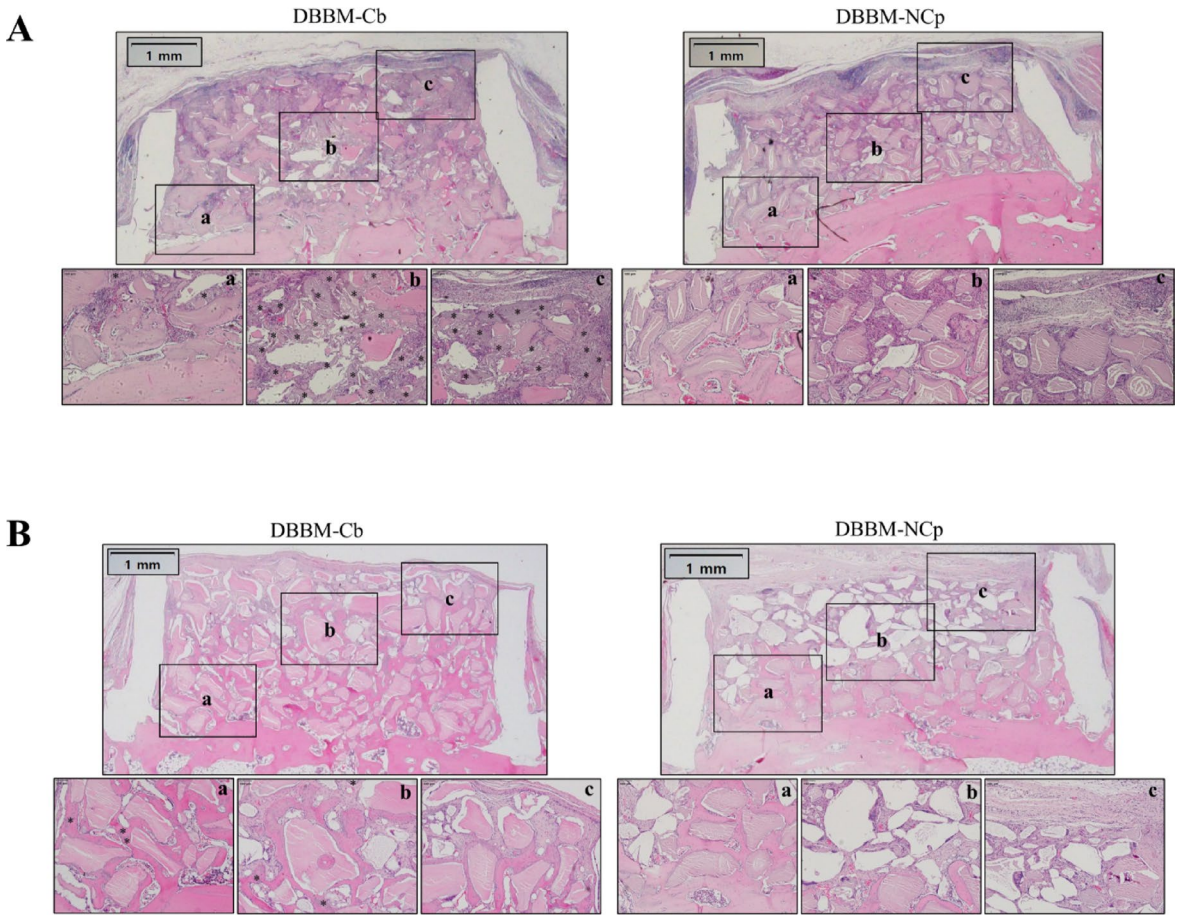

Fig. 4. Representative histological images of the vertically augmented area. Specimens have been stained using hematoxylin and eosin. The rectangular boxes labeled (a), (b), and (c) in the upper panels correspond to the respective high-magnification views shown below. (**A**) Histological sections of vertically augmented tissues at 3 weeks after surgery. In the DBBM-Cb group, residual collagen is observed. In contrast, minimal residual collagen was detected in the DBBM-NCp group, indicating more rapid scaffold degradation and active remodeling. (**B**) Histological sections of vertically augmented tissues at 5 weeks after surgery. The upper region reveals maintained DBBM deposition in the DBBM-Cb group. *DBBM-NCp* deproteinized bovine bone mineral with non-crosslinked porcine collagen (Bio-Oss Collagen, Geistlich Pharma, Switzerland), *DBBM-Cb* deproteinized bovine bone mineral with crosslinked bovine collagen (A-Oss Collagen, Osstem, Republic of Korea).

advanced tissue engineering strategies—including the incorporation of growth factors or stem cells—warrants further investigation. Such applications could expand its utility beyond conventional bone grafting, enabling personalized regenerative approaches in complex clinical scenarios. Despite these advantages, chemically cross-linked collagen carries recognized limitations, including the risk of cytotoxicity and inflammatory responses in surrounding tissues[35]. Nevertheless, in the present study we observed no adverse responses, and histology revealed no abnormal inflammatory reactions.

The experimental design (Fig. 6) employed two validated rabbit calvarial models, which minimize confounding factors such as masticatory loading and provide a flat bone surface for standardized preparation. As in previous studies, these vertical augmentation and critical-sized defect models were used to facilitate reproducibility and comparability across experimental sites[36,37]. Early histologic and micro-CT analyses revealed distinct bone formation patterns between the two materials[37–39], supporting the usefulness of early-phase assessment for evaluating graft performance.

Micro-CT provided high-resolution, three-dimensional volumetric data[23], whereas histologic analysis revealed cellular-level details, enabling comprehensive evaluation of bone regeneration[40]. Findings from both methods were consistent, reinforcing the reliability of the observed outcomes.

Despite promising results, this study had some limitations. The use of an animal model may limit the direct translatability to human clinical settings, given the various defect conditions, and the relatively small sample size weakens the statistical strength of the findings. Additionally, the 12-week follow-up period may not fully reflect long-term remodeling and resorption. The follow-up periods were set differently for each model due to their distinct biological characteristics: short intervals (3 and 5 weeks) in the vertical augmentation model to capture early dimensional changes without supporting walls, and longer intervals (6 and 12 weeks) in the calvarial defect

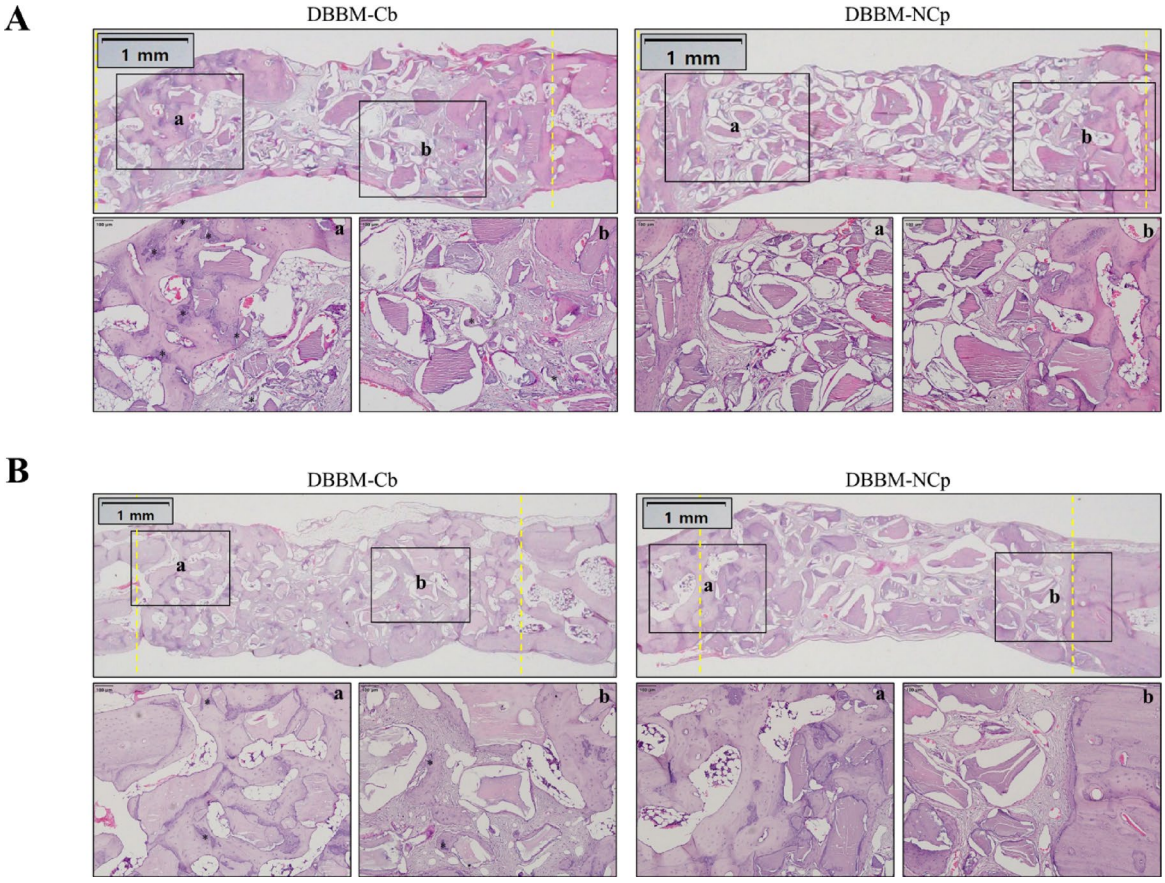

Fig. 5. Representative histological images of the defect areas. Specimens have been stained using hematoxylin and eosin. The rectangular boxes labeled a and b in the upper panels correspond to the respective high-magnification views shown below. (**A**) Histological sections of defect tissues at 6 weeks after surgery. Newly formed bone, residual graft material, and connective tissue are observed. (**B**) Histological sections of defect tissues at 12 weeks after surgery. DBBM-Cb and DBBM-NCp groups show continuous new bone formation and integration throughout the defect area. *DBBM-NCp* deproteinized bovine bone mineral with non-crosslinked porcine collagen (Bio-Oss Collagen, Geistlich Pharma, Switzerland), *DBBM-Cb* deproteinized bovine bone mineral with crosslinked bovine collagen (A-Oss Collagen, Osstem, Republic of Korea).

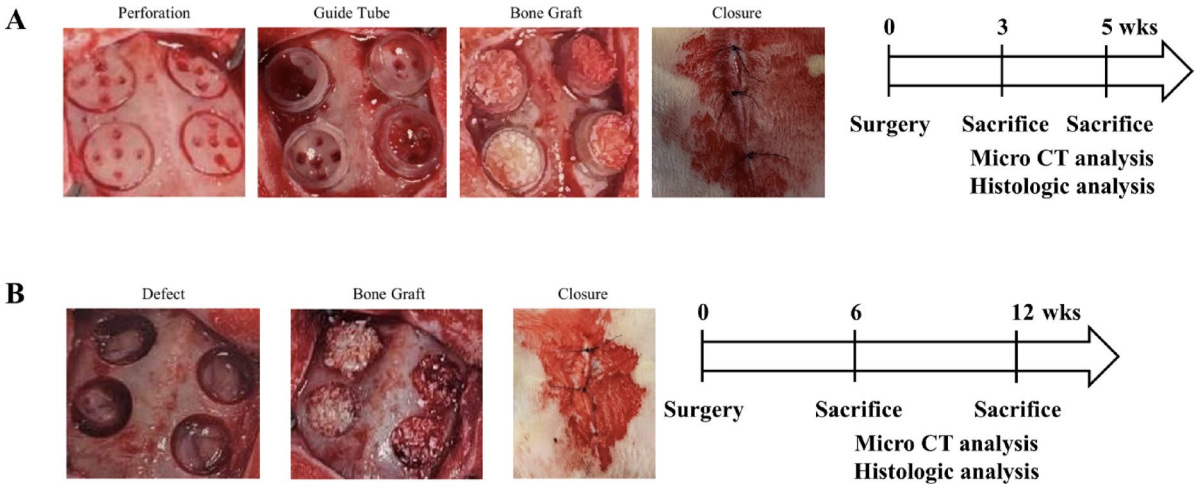

Fig. 6. Experimental animal models and procedure. (**A**) Calvarial augmentation model. (**B**) Calvarial defect model.

model with circumferential bony walls and greater stability, which limited direct comparison between the two models. Further studies, including clinical trials, with larger cohorts and extended timeframes are needed to validate these findings.

Within the limitations of the study, DBBM-Cb demonstrated superior osteoconductive properties, prolonged structural integrity, and greater bone regeneration compared to DBBM-NCp, suggesting its potential as a more effective material for bone augmentation procedures.

Materials and methods

Animals

Twenty-four male New Zealand White rabbits (weight, 2.5–3.0 kg; age, 15 weeks) were used in this study. Animals were purchased from DooYeol Biotech (Seoul, Republic of Korea) and allowed a 2-week acclimation period prior to experimentation. They were housed individually under standardized environmental conditions with ad libitum access to food and water. All animal procedures, including selection, housing, and surgical interventions, were reviewed and approved by the Osstem Implant Institutional Animal Care and Use Committee (Approval No. OST-IACUC2310). All procedures were performed in accordance with the relevant guidelines and regulations, a modified version of the Animal Research: Reporting of In Vivo Experiments (ARRIVE) guidelines.

Field emission scanning electron microscopy

To assess the surface morphology of the bone-graft materials, field emission scanning electron microscopy (FE-SEM; JSM-7610FPlus; JEOL Ltd., Akishima, Tokyo, Japan) was performed at an acceleration voltage of 15 kV. Imaging was conducted at magnifications of 50×, and 30,000× (Fig. 1). For improved image clarity and electrical conductivity, the samples were sputter-coated twice with platinum at 30 mA for 150 s each.

Study design

In this study, two distinct in vivo models—a calvarial augmentation model and a calvarial defect model—were used to evaluate the osteoconductive properties of the graft materials (Fig. 6).

In the calvarial augmentation model, four circular recesses (6 mm in diameter) were created on the parietal bone of each rabbit ($N = 12$ sites, respectively). Guide tubes (diameter, 6 mm; height, 3 mm) were fixed over the recesses using bone adhesive (GluStitch®; Glustitch Inc., Vancouver, Canada), and subsequently filled with either DBBM-Cb or DBBM-NCp. Rabbits were euthanized at 3 and 5 weeks after surgery using CO_2 inhalation, and microcomputed tomography (micro-CT) and histological analyses were performed.

In the calvarial defect model, four standardized defects (diameter, 6 mm) were created on the parietal bone. Each defect was filled with one of the two bone graft materials ($N = 12$ sites, respectively). Rabbits were euthanized at 6 and 12 weeks postoperatively using CO_2 inhalation, and micro-CT and histological evaluations were performed.

Surgical protocol

Prior to surgery, rabbits were anesthetized with an intramuscular injection of a mixture containing tiletamine and zolazepam (10 mg/kg) and xylazine (5 mg/kg). Next, the surgical site was shaved and disinfected using povidone-iodine solution and 70% ethanol. A 2-cm midline incision was made in the calvarial skin along the sagittal suture, and the underlying periosteum was incised along the same line to expose the parietal bone. Surgical procedures were performed according to the protocols for either the calvarial defect or vertical augmentation models. Two graft materials were bilaterally implanted in the calvarial bones of each rabbit. The side receiving each material was randomly determined to eliminate site-specific bias. After bone grafting, the periosteum was closed using absorbable sutures (Maxon®; Covidien, Dublin, Ireland), and the skin was closed using non-absorbable sutures (Blue Nylon; AILEE Co., Busan, Republic of Korea). Postoperatively, the surgical site was disinfected again using povidone-iodine solution. Postoperative analgesia and antibiotic prophylaxis were provided via intramuscular injection of meloxicam (0.2 mg/kg) and enrofloxacin (Baytril®, 0.1 ml/kg; Bayer Vital, Germany), respectively. Animals were closely monitored for signs of distress or abnormal behavior, including feeding patterns and activity levels, until the time of euthanasia. Harvested tissue specimens were fixed in 4% paraformaldehyde solution for subsequent micro-CT and histological analyses.

Micro-CT image analysis

New bone volume and the amount of residual graft material were quantified using micro-CT (SMX-225CT, Shimadzu Co., Kyoto, Japan). Scanning was performed at 110 kV and 50 μA using a metal filter, with a pixel size of 8 μm. Image reconstruction was performed using InspeXio software (Ver. 5.0.0.0; Shimadzu Co., Kyoto, Japan) in accordance with the manufacturer's instructions.

The region of interest was defined as the space in which the bone graft material was placed and where new bone formation and residual graft volume were evaluated. In the calvarial defect model, the region of interest was defined as the area surrounding the guide tube in the defect area (Fig. 3A).

Histological analysis

Fixed tissue samples were decalcified in 4% ethylenediaminetetraacetic acid solution for 30 days. Following decalcification, the specimens were dehydrated using a graded series of ethanol and cleared using xylene. The samples were then embedded in paraffin, and 4-μm thick sections were obtained. Histological evaluation was performed after hematoxylin and eosin (H&E) staining (Figs. 4 and 5).

Statistical analysis

All data are presented as mean ± standard deviation. Statistical analyses were performed using Microsoft Excel (Microsoft Corp., Redmond, WA, USA). Statistical comparisons between two groups were performed using an unpaired Student's t-test. Statistical significance was set at $P < 0.05$.

Data availability

All data generated or analyzed during this study are included in this published article.

Received: 11 August 2025; Accepted: 27 November 2025
Published online: 05 December 2025

References

1. Chappuis, V., Cavusoglu, Y., Buser, D. & von Arx, T. Lateral ridge augmentation using autogenous block grafts and guided bone regeneration: A 10-year prospective case series study. *Clin. Implant Dent. Relat. Res.* **19**, 85–96 (2017).
2. Nystrom, E., Kahnberg, K. E. & Gunne, J. Bone grafts and Branemark implants in the treatment of the severely resorbed maxilla: A 2-year longitudinal study. *Int. J. Oral Maxillofac. Implants* **8**, 45–53 (1993).
3. Norton, M. R., Odell, E. W., Thompson, I. D. & Cook, R. J. Efficacy of bovine bone mineral for alveolar augmentation: A human histologic study. *Clin. Oral Implants Res.* **14**, 775–783. https://doi.org/10.1046/j.0905-7161.2003.00952.x (2003).
4. Mendoza-Azpur, G., de la Fuente, A., Chavez, E., Valdivia, E. & Khouly, I. Horizontal ridge augmentation with guided bone regeneration using particulate xenogenic bone substitutes with or without autogenous block grafts: A randomized controlled trial. *Clin. Implant Dent. Relat. Res.* **21**, 521–530. https://doi.org/10.1111/cid.12740 (2019).
5. Zitzmann, N. U., Naef, R. & Scharer, P. Resorbable versus nonresorbable membranes in combination with Bio-Oss for guided bone regeneration. *Int. J. Oral Maxillofac. Implants* **12**, 844–852 (1997).
6. Cucchi, A. et al. Complication, vertical bone gain, volumetric changes after vertical ridge augmentation using customized reinforced PTFE mesh or Ti-mesh. A non-inferiority randomized clinical trial. *Clin. Oral Implants Res.* **35**, 1616–1639. https://doi.org/10.1111/clr.14350 (2024).
7. Ronda, M., Rebaudi, A., Torelli, L. & Stacchi, C. Expanded vs. dense polytetrafluoroethylene membranes in vertical ridge augmentation around dental implants: A prospective randomized controlled clinical trial. *Clin. Oral Implants Res.* **25**, 859–866. https://doi.org/10.1111/clr.12157 (2014).
8. McAllister, B. S. & Haghighat, K. Bone augmentation techniques. *J .Periodontol.* **78**, 377–396. https://doi.org/10.1902/jop.2007.060048 (2007).
9. Park, J. I. et al. Space maintenance using crosslinked collagenated porcine bone grafted without a barrier membrane in one-wall intrabony defects. *J. Biomed. Mater. Res. B Appl. Biomater.* **102**, 1454–1461 (2014).
10. Li, J. et al. Repair of rabbit radial bone defects using true bone ceramics combined with BMP-2-related peptide and type I collagen. *Mater. Sci. Eng. C* **30**, 1272–1279 (2010).
11. Zigdon, H., Lewinson, D., Bick, T. & Machtei, E. E. Vertical bone augmentation using different osteoconductive scaffolds combined with barrier domes in the rat calvarium. *Clin. Implant Dent. Relat. Res.* **16**, 138–144. https://doi.org/10.1111/j.1708-8208.2012.00452.x (2014).
12. Kato, E., Lemler, J., Sakurai, K. & Yamada, M. Biodegradation property of beta-tricalcium phosphate-collagen composite in accordance with bone formation: a comparative study with Bio-Oss Collagen® in a rat critical-size defect model. *Clin. Implant Dent. Relat. Res.* **16**, 202–211 (2014).
13. Davidenko, N. et al. Control of crosslinking for tailoring collagen-based scaffolds stability and mechanics. *Acta Biomater.* **25**, 131–142. https://doi.org/10.1016/j.actbio.2015.07.034 (2015).
14. Lee, J. C. et al. Optimizing collagen scaffolds for bone engineering: Effects of cross-linking and mineral content on structural contraction and osteogenesis. *J. Craniofac. Surg.* **26**, 1992–1996 (2015).
15. Oryan, A., Kamali, A., Moshiri, A., Baharvand, H. & Daemi, H. Chemical crosslinking of biopolymeric scaffolds: Current knowledge and future directions of crosslinked engineered bone scaffolds. *Int. J. Biol. Macromol.* **107**, 678–688 (2018).
16. Jarman-Smith, M. L. et al. Porcine collagen crosslinking, degradation and its capability for fibroblast adhesion and proliferation. *J. Mater. Sci. Mater. Med.* **15**, 925–932 (2004).
17. Angele, P. et al. Influence of different collagen species on physico-chemical properties of crosslinked collagen matrices. *Biomaterials* **25**, 2831–2841. https://doi.org/10.1016/j.biomaterials.2003.09.066 (2004).
18. Robert, L., Aloy-Prosper, A. & Arias-Herrera, S. Vertical augmentation of the atrofic posterior mandibular ridges with onlay grafts: Intraoral blocks vs. guided bone regeneration. Systematic review. *J. Clin. Exp. Dent.* **15**, e357–e365. https://doi.org/10.4317/jced.60294 (2023).
19. Alotaibi, F. F., Rocchietta, I., Buti, J. & D'Aiuto, F. Comparative evidence of different surgical techniques for the management of vertical alveolar ridge defects in terms of complications and efficacy: A systematic review and network meta-analysis. *J. Clin. Periodontol.* **50**, 1487–1519. https://doi.org/10.1111/jcpe.13850 (2023).
20. Donos, N., Akcali, A., Padhye, N., Sculean, A. & Calciolari, E. Bone regeneration in implant dentistry: Which are the factors affecting the clinical outcome?. *Periodontol.* **2000**(93), 26–55 (2023).
21. Blanco, J., Alonso, A. & Sanz, M. Long-term results and survival rate of implants treated with guided bone regeneration: A 5-year case series prospective study. *Clin. Oral Implant Res.* **16**, 294–301 (2005).
22. Lee, D. W. et al. Longitudinal comparative study on osteogenic capacity using two collagenated xenografts in artificial bone defects in beagles. *Sci. Rep.* **15**, 10408. https://doi.org/10.1038/s41598-025-94284-8 (2025).
23. Lim, H. C., Paeng, K. W., Jung, U. W. & Benic, G. I. Vertical bone augmentation using collagenated or non-collagenated bone substitute materials with or without recombinant human bone morphogenetic protein-2 in a rabbit calvarial model. *J. Periodontal Implant Sci.* **53**, 429–443. https://doi.org/10.5051/jpis.2204240212 (2023).
24. Di Stefano, D. A., Orlando, F., Ottobelli, M., Fiori, D. & Garagiola, U. A comparison between anorganic bone and collagen-preserving bone xenografts for alveolar ridge preservation: Systematic review and future perspectives. *Maxillofac. Plast. Reconstr. Surg.* **44**, 24 (2022).
25. Liu, Q. et al. Comparison of in vitro biocompatibility of NanoBone® and BioOss® for human osteoblasts. *Clin. Oral Implant Res.* **22**, 1259–1264 (2011).
26. Keil, C., Gollmer, B., Zeidler-Rentzsch, I., Gredes, T. & Heinemann, F. Histological evaluation of extraction sites grafted with Bio-Oss collagen: Randomized controlled trial. *Ann. Anat. Anat. Anz.* **237**, 151722 (2021).
27. Wang, J., Cui, W., Zhao, Y., Lei, L. & Li, H. Clinical and radiographic evaluation of Bio-Oss granules and Bio-Oss Collagen in the treatment of periodontal intrabony defects: A retrospective cohort study. *J. Appl. Oral Sci.* **32**, e20230268. https://doi.org/10.1590/1678-7757-2023-0268 (2024).
28. Araujo, M. G. & Lindhe, J. Ridge preservation with the use of Bio-Oss collagen: A 6-month study in the dog. *Clin. Oral Implants Res.* **20**, 433–440. https://doi.org/10.1111/j.1600-0501.2009.01705.x (2009).

29. Rothamel, D. et al. Biodegradation of differently cross-linked collagen membranes: An experimental study in the rat. *Clin. Oral Implants Res.* **16**, 369–378. https://doi.org/10.1111/j.1600-0501.2005.01108.x (2005).
30. Lee, J. T., Lee, S. H., Choi, B. S. & Kim, S. Comparison of four bone substitute types in sinus augmentation with perforated Schneiderian membrane: An experimental study. *J. Periodontol.* https://doi.org/10.1002/JPER.24-0663 (2025).
31. Zhu, M., Duan, B., Hou, K., Mao, L. & Wang, X. A comparative in vitro and in vivo study of porcine-and bovine-derived non-cross-linked collagen membranes. *J. Biomed. Mater. Res. B Appl. Biomater.* **111**, 568–578 (2023).
32. Ghodbane, S. A. & Dunn, M. G. Physical and mechanical properties of cross-linked type I collagen scaffolds derived from bovine, porcine, and ovine tendons. *J. Biomed. Mater. Res. Part A* **104**, 2685–2692 (2016).
33. Tal, H., Kozlovsky, A., Artzi, Z., Nemcovsky, C. E. & Moses, O. Long-term bio-degradation of cross-linked and non-cross-linked collagen barriers in human guided bone regeneration. *Clin. Oral Implants Res.* **19**, 295–302. https://doi.org/10.1111/j.1600-0501.2007.01424.x (2008).
34. Nowotny, K. & Grune, T. Degradation of oxidized and glycoxidized collagen: Role of collagen cross-linking. *Arch. Biochem. Biophys.* **542**, 56–64. https://doi.org/10.1016/j.abb.2013.12.007 (2014).
35. Veríssimo, D. et al. Polyanionic collagen membranes for guided tissue regeneration: Effect of progressive glutaraldehyde cross-linking on biocompatibility and degradation. *Acta Biomater.* **6**, 4011–4018 (2010).
36. Park, J.-B., Kim, I., Lee, W. & Kim, H. Evaluation of the regenerative capacity of stem cells combined with bone graft material and collagen matrix using a rabbit calvarial defect model. *J. Periodontal Implant Sci.* **53**, 467 (2023).
37. Slotte, C., Lundgren, D. & Sennerby, L. Bone morphology and vascularization of untreated and guided bone augmentation-treated rabbit calvaria: evaluation of an augmentation model. *Clin. Oral Implant Res.* **16**, 228–235 (2005).
38. Schlund, M. et al. Rabbit calvarial and mandibular critical-sized bone defects as an experimental model for the evaluation of craniofacial bone tissue regeneration. *J. Stomatol. Oral Maxillofac. Surg.* **123**, 601–609 (2022).
39. Kim, D. H., Cha, J. K., Song, Y. W., Woo, K. M. & Jung, U. W. Bone augmentation using small molecules with biodegradable calcium sulfate particles in a vertical onlay graft model in the rabbit calvarium. *J. Biomed. Mater. Res. B Appl. Biomater.* **108**, 1343–1350 (2020).
40. Ozer, T. et al. Locally administrated single-dose teriparatide affects critical-size rabbit calvarial defects: A histological, histomorphometric and micro-CT study. *Acta Orthop. Traumatol. Turc.* **53**, 478–484. https://doi.org/10.1016/j.aott.2019.08.007 (2019).

Author contributions

Conceptualization: Young-Dan Cho; Formal analysis: Narasaem Lee, Semin Kim; Investigation: Hee-seung Han, Hyunkyung Kim, Semin Kim; Methodology: Sungtae Kim, Young-Dan Cho; Project administration: Sungtae Kim, Young-Dan Cho; Writing—original draft: Hee-seung Han, Hyunkyung Kim, Narasaem Lee, Sungtae Kim, Young-Dan Cho; Writing—review and editing: Sungtae Kim, Young-Dan Cho; Hee-seung Han, Hyunkyung Kim contributed equally as first authors.

Funding

This work was supported by the Creative-Pioneering Researchers Program through Seoul National University, Bio & Medical Technology Development Program of the National Research Foundation (NRF) funded by the Korean government (MSIT) (No. RS-2022-NR067350 and RS-2024-00349549), the Technology development Program (RS-2023-00268594) funded by the Ministry of SMEs and Startups (MSS, Republic of Korea), and Korea Health Technology R&D Project through the Korea Health Industry Development Institute (KHIDI), funded by the Ministry of Health & Welfare, Republic of Korea (No. HI23C0544).

Declarations

Competing interests

The authors declare no competing interests.

Ethics declarations

All animal procedures, including selection, housing, and surgical interventions, were reviewed and approved by the Osstem Implant Institutional Animal Care and Use Committee (Approval No. OST-IACUC2310). All procedures were performed in accordance with a modified version of the Animal Research: Reporting of In Vivo Experiments (ARRIVE) guidelines.

Additional information

Supplementary Information The online version contains supplementary material available at https://doi.org/10.1038/s41598-025-30824-6.

Correspondence and requests for materials should be addressed to Y.-D.C.

Reprints and permissions information is available at www.nature.com/reprints.

Publisher's note Springer Nature remains neutral with regard to jurisdictional claims in published maps and institutional affiliations.

Open Access This article is licensed under a Creative Commons Attribution-NonCommercial-NoDerivatives 4.0 International License, which permits any non-commercial use, sharing, distribution and reproduction in any medium or format, as long as you give appropriate credit to the original author(s) and the source, provide a link to the Creative Commons licence, and indicate if you modified the licensed material. You do not have permission under this licence to share adapted material derived from this article or parts of it. The images or other third party material in this article are included in the article's Creative Commons licence, unless indicated otherwise in a credit line to the material. If material is not included in the article's Creative Commons licence and your intended use is not permitted by statutory regulation or exceeds the permitted use, you will need to obtain permission directly from the copyright holder. To view a copy of this licence, visit http://creativecommons.org/licenses/by-nc-nd/4.0/.

© The Author(s) 2025